SELECTED NEW RAPIDLY QUENCHED SOFT MAGNETIC SYSTEMS

P. Švec Jr.[1], I. Janotova[1], I. Mat'ko[1], J. Zigo[1], J. Marcin[2], D. Janičkovič[1], I. Škorvánek[2], P. Švec[1]

[1] *Institute of Physics, Slovak Academy of Sciences, Bratislava, Slovakia,*
[2] *Institute of Experimental Physics, Slovak Academy of Sciences, Košice, Slovakia*
E-mail: peter.svec@savba.sk

Received 15 May 2016; accepted 23 May 2016

1. Introduction

Nowadays the well-known classical rapidly quenched nanocrystalline soft magnetic materials such as FINEMET [1], NANOPERM [2] and HITPERM [3] are seconded by new intensely investigated systems. Among these a special attention is put on materials with increased saturation magnetic flux density exceeding the values of 1.8T while preserving low coercivity [4, 5]. Technically it is also important that the materials can be exposed to long-term operating temperatures ranging well above ambient, exceeding 500K or even more. Diverse new systems based on Fe-B with additions of Co, Cu, C, P and other elements were developed and tested. Successful compositional and processing design has lead to a new class of so-called NANOMET alloys which fulfill requirements posed on modern soft magnetic materials [6-9].

The potential of replacement of rare-earth elements in FINEMET, NANOPERM and HITPERM alloy systems by more abundant elements has been successfully shown on NANOPERM-like Fe-B system with small additions of Sn [10, 11]. The drive for high saturation magnetic flux density is inevitably related to increase of content of ferromagnetic elements in the alloy, in this case Fe, to the limit of glass formability given by the minimal content of glass-forming element, i. e. B. Thus our work is focused on rapidly quenched Fe-Sn-B systems with decreased B content and addition of Sn at the expense of Fe in order to form nanocrystalline grains from as-cast amorphous structure by suitable annealing.

The reason for selection of Fe-B system is the fact that it represents one of the most studied amorphous systems. In addition, atomic radii of Fe and Sn atoms are favorable for incorporation of Sn in the Fe-rich amorphous phase in spite of a rather low melting point of Sn as compared to Fe. Another reason for interest in Fe-Sn-B or Fe-Co-Sn-B based systems is the elimination of conventional nanocrystal forming elements belonging to the rare-earth group (Nb, Nd, etc.), which is in accord with recent EU policy related to the use of critical raw elements; furthermore, Sn is an abundant and inexpensive alloying element.

Hereby we present selected results related to the preparation, structure and some properties of rapidly quenched $Fe_{(85-x)}Sn_xB_{15}$, x=0, 3.5, 5 and 7 with emphasis on x=7.

2. Experimental

Amorphous ribbons were prepared by the planar flow casting from previously prepared master alloys with selected chemical composition. The samples 6 mm wide and ~20 μm thick were linearly heated with 10K/min heating rate and isothermally annealed at several selected temperatures. The transformation from as-cast amorphous state was monitored using the measurements of temperature dependencies of relative electrical resistivity *R(T)/R(*300K) using four-probe method in planar contact furnace in vacuum; the same furnace was used for thermal treatment of samples for transmission electron microscopy (JEOL 2000FX at 200kV) and x-ray diffraction using Bruker D8 Advance diffractometer with parallel incident beam (Cu K_alpha radiation 40kV/35mA) and LiF monochromator in the diffracted beam. Magnetic hysteresis loops were acquired using a Forster type B-H loop tracer based on flux-gate magnetometer.

3. Results and discussion

Transformation of as-cast Fe-Sn-B with different Sn content is shown in Fig. 1 using temperature dependence of relative electrical resistivity during linear heating. The decrease of electrical resistivity above 650K for all samples corresponds to formation of bcc-Fe(Sn) crystalline phase from amorphous matrix. The onset temperatures of this phase transformation in alloys containing Sn are slightly higher than that observed in Sn-free $Fe_{85}B_{15}$. Crystallization of the amorphous remains takes place above 750K and is reflected by a sharp drop of electrical resistivity. It is to be noted that the temperature interval between the first and the second crystallization reactions in all cases is higher than 100K, which provides a conveniently broad interval for thermal processing and controlled formation of ferromagnetic bcc-Fe)Sn) phase.

The amorphous state of a-cast samples and the formation of bcc-Fe(Sn), which has a higher lattice parameter than pure bcc-Fe, is proven by x-ray diffraction of samples containing 7 at.% Sn shown in Fig. 2. This phase remains as the only crystalline phase present in amorphous matrix up to the temperatures where the second crystallization takes place, leading to formation of additional peaks, all corresponding to Sn-containing phases - hexagonal Fe(Sn) and hexagonal Fe_3Sn_2. Formation of Fe-B borides takes place above 950K, in accord with the corresponding phase diagram [12].

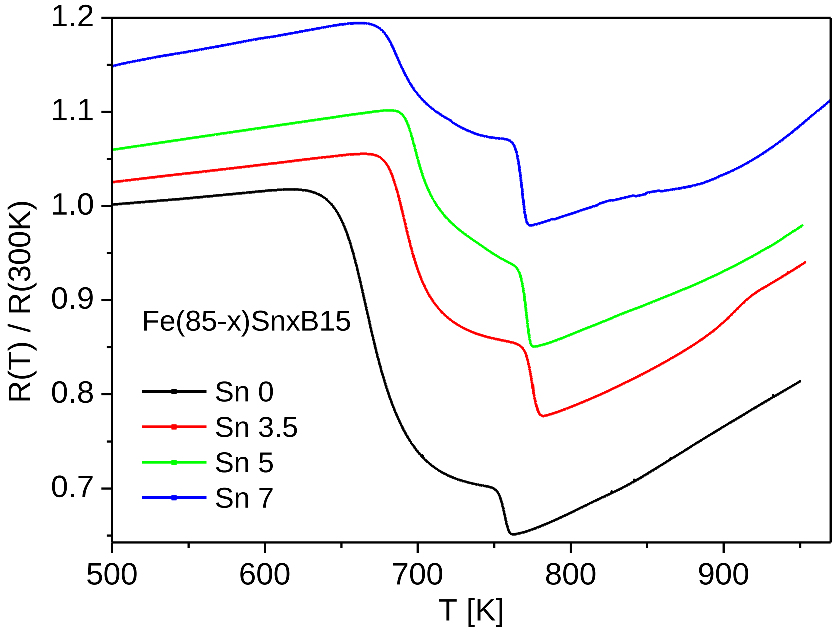

Fig.1: *Temperature dependence of normalized electrical resistivity for rapidly quenched* $Fe_{(85-x)}Sn_xB_{15}$ *system for x= 0, 3.5, 5 and 7; linear heating 10K/min. The curves are shifted vertically for clarity.*

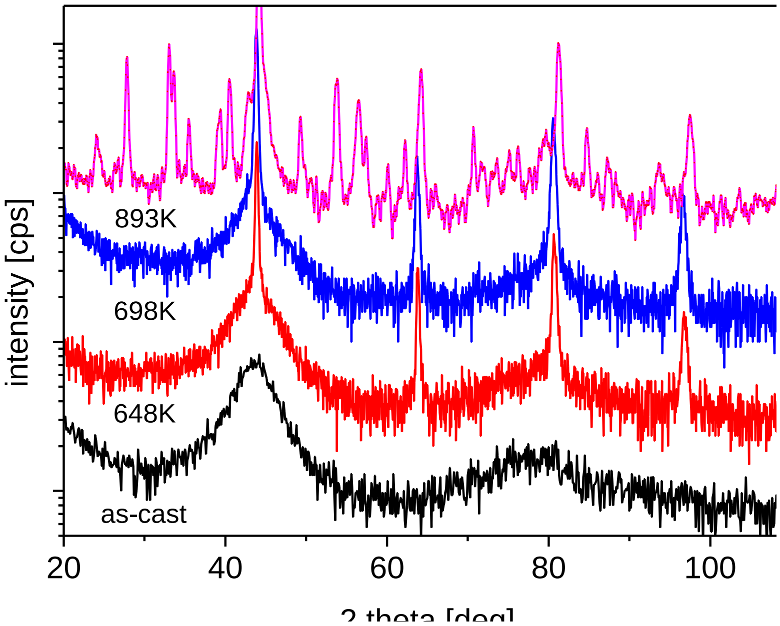

Fig.2: *X-ray diffraction patterns of $Fe_{78}Sn_7B_{15}$ in as-cast state and after isothermal annealing for 30 minutes at indicated temperatures. Maxima formed at 648 and 698K correspond to bcc-Fe(Sn); additional maxima formed at 893K correspond to hexagonal Fe(Sn) and hexagonal Fe_3Sn_2. The curves are shifted vertically for clarity.*

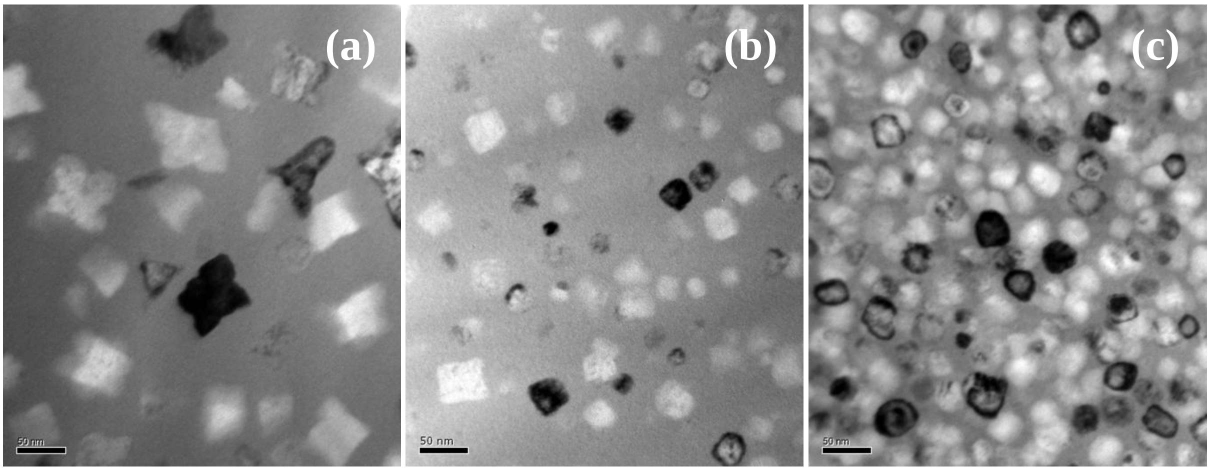

Fig.3: *Microstructure of $Fe_{81.5}Sn_{3.5}B_{15}$, $Fe_{80}Sn_5B_{15}$ and $Fe_{78}Sn_7B_{15}$ in (a), (b) and (c), respectively, annealed to the temperature of maximal rate of the first decrease of relative resistivity in Fig.1. Scale bar in all cases is 50nm.*

The morphology of phases formed from amorphous matrix during the first crystallization stage is shown in Fig. 3 for different Sn content. While in pure $Fe_{85}B_{15}$ amorphous alloy dendritic-like grains about 150nm in size are formed [5], increase of Sn content leads to refinement of the grain sizes as well as to the change of morphology of the grains. Tiny dendritic-like ~50nm large crystals observed for 3.5 at. % Sn change into significantly smaller grains of rhomboedric shape for 5 at. % Sn. Nearly spherical 25-50nm sized structures well separated from each other by the remaining amorphous matrix are formed for 7 at. % Sn. The morphology is similar to that observed in classical nanocrystalline alloys mentioned in the Introduction, however, without rare-earth grain refiners [13].

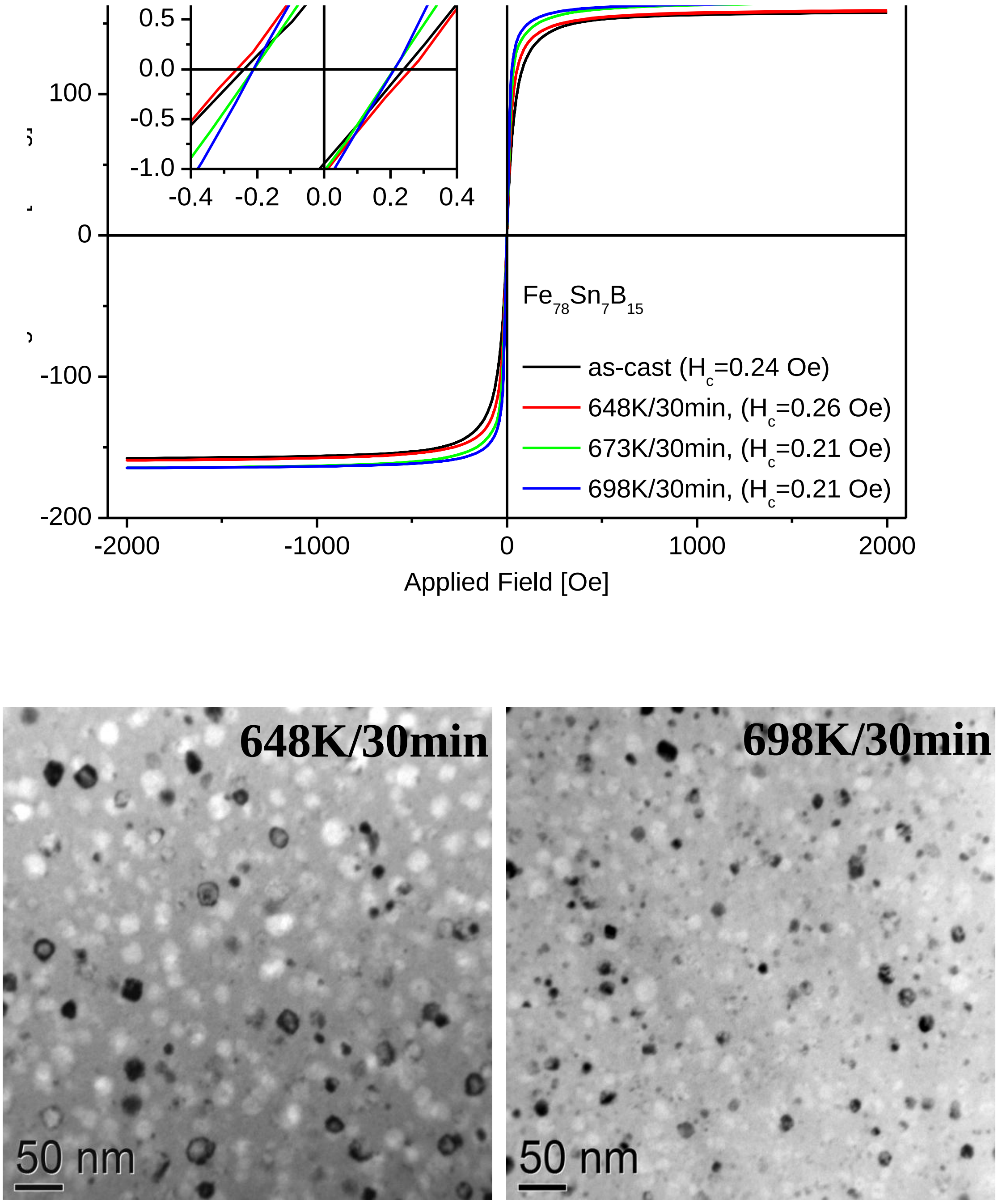

Fig.4: *Quasistatic hysteresis loops of as-cast and annealed $Fe_{78}Sn_7B_{15}$ (top); inset shows the behaviour of magnetization at low applied fields for determination of coercivity H_c. TEM images illustrate the corresponding size, content and distribution of the nanocrystalline bcc-Fe(Sn) grains in amorphous matrix formed after annealing at indicated temperatures.*

Magnetic hysteresis loops shown for $Fe_{78}Sn_7B_{15}$ in Fig. 4 show at the same time high values of magnetization for as-cast and nanocrystalline samples as well as low magnetic coercivity values. It is interesting to note that the coercivity values decrease only slightly with proceeding nanocrystallization. However, samples annealed into nanocrystalline state are structurally stable and, with respect to high Curie temperature of the annealed alloy, which lies above the temperature of the second crystallization stage, allow applications at temperatures exceeding 600K. Higher annealing temperature (TEM images in Fig. 4) leads to further refinement of the nano sized grains without their tendency to coarsening even after prolonged annealing. This effect suggests that the formation of nanocrystalline grains is thermodynamic and not kinetic effect; the grain growth stops after attaining a definite size and is not simply kinetically arrested due to annealing for a short time only, which is the case of Fe-B-Cu [4,5].

4. Conclusions

Substitution of Fe by small amounts of Sn in amorphous $Fe_{85}B_{15}$ system leads to formation of amorphous structure which transforms partly into nanocrystalline grains stable until 750K. Increased Sn content up to 7 at. % enhances nanocrystallization and leads to a large number of spherical grains distributed evenly in the remaining amorphous matrix. The nanocrystalline phase formed in the first crystallization stage was identified as bcc-Fe(Sn). In combination with amorphous remains the alloy forms a composite structure with high saturation magnetization and low values of magnetic coercivity which can be further tuned by proper thermal treatment.

Acknowledgement

The authors would like to acknowledge the support of the project CEKOMAT II, ITMS 26240120020, supported by the Research and Development Operational Program funded by the ERDF.

References:

[1] Y. Yoshizawa, S. Oguma, K. Yamauchi, J. Appl. Phys. **64** (1988) 6044.
[2] K. Suzuki, A. Makino, A. Inoue, T. Masumoto, J. Appl. Phys. **70** (1991) 6232.
[3] M. A. Willard et al., J. Appl. Phys. **84** (1998) 6773.
[4] M. Ohta, Y. Yoshizawa, J. Magn. Magn. Mater. **320** (2008) 750.
[5] P. Svec et al., IEEE Trans. Magn. **46** (2010) 408.
[6] P. Sharma, X. Zhang, Y. Zhang, A. Makino, Scripta Mater. **95** (2015) 3.
[7] K. Takenaka et al., J. Magn. Magn. Mater. **401** (2016) 479.
[8] I. Janotova et al., J. of Superconductivity and Novel Magnetism **26** (2013) 793.
[9] I. Janotova et al., J. of Alloys and Compounds **615** (2015) S198.
[10] E. Illekova et al., J. of Alloys and Compounds **509** (2011) S46.
[11] I. Matko et al., J. of Alloys and Compounds **615** (2015) S462.
[12] H. Okamoto / Phase Diagrams of Binary Iron Alloys (1993) 93-101.
[13] G. Herzer, Acta Mater. **61** (2013) 718.